Int. J. Multiphase Flow Vol. 17, No. 2, pp. 283–289, 1991
Printed in Great Britain

0301-9322/91 $3.00 + 0.00
Pergamon Press/Elsevier

BRIEF COMMUNICATION

HYSTERESIS EFFECT IN FLOODING

G. P. CELATA, M. CUMO, G. E. FARELLO and T. SETARO
ENEA TERM/ISP-Casaccia, Via Anguillarese 301, Roma, Italia

(Received 27 February 1990; in revised form 14 September 1990)

INTRODUCTION

The present brief communication refers to a flooding experiment aimed at studying the hysteresis phenomenon. The hysteresis effect occurs when, once the onset of the flooding condition has been reached, either the liquid or the gas mass flow rate is decreased with the aim of restoring countercurrent flow. The flooding condition persists until the reduced flow rate is decreased with the aim of restoring countercurrent flow. The flooding condition persists until the reduced flow rate reaches a value much lower than the flooding liquid flow rate. This condition is called the "deflooding point". Hewitt & Wallis (1966) and Becker & Letzter (1978) investigated the hysteresis effect by reducing the gas flow rate while keeping the liquid flow rate constant. They found that the values of the deflooding gas velocity were lower with respect to the flooding ones and that the hysteresis effect became less important when decreasing the liquid flow rate. Clift *et al.* (1966) made a systematic study of hysteresis and also investigated the condition of hysteresis with a decreasing liquid flow rate and constant gas flow rate. Again, the value of the deflooding liquid flow rate was shown to be lower than the flooding liquid flow rate.

In the present experiments, the hysteresis effect was studied keeping the gas flow rate constant during the tests, whilst the liquid flow rate was varied.

EXPERIMENTAL SETUP AND PROCEDURES

The experimental tests were carried out at atmospheric pressure with an air–water loop, named *FLEX*, as shown in figure 1. The test section is made of Plexiglas, in order to obtain visual information and to verify the correct performing of the tests. The full vertical test section lengths are 500 and 405 mm for inner test channel diameters of 20 and 16.2 mm, respectively. The instrumentation consists of thermocouples and pressure transducers at the inlet of the test section for the measurement of the gas thermodynamic conditions. Demineralized water is supplied from the top of the test section through a circular weir; its flow rate is measured using turbine flowmeters. Air is supplied from the bottom of the test section (lower plenum); its flow rate is measured using a calibrated sonic disk.

Before entering the test section, air flows through a vertical 7° convergent duct connected to the test channel. This enables the gas to pass through the test channel with an already developed and steady velocity profile. It was observed that the wall of the convergent channel was always wetted by a continuous liquid film. The gas inlet section can be therefore classified as smooth. Entrained water is separated from the gas–water mixture in a high-efficiency air–water separator, placed at the top end of the test channel (just above the water injection point), and collected in a small tank. The average value of the entrained water mass flow rate is obtained by weighing the water collected during the test. In order to minimize scattering in the data measurements, the collecting time was always > 2 min.

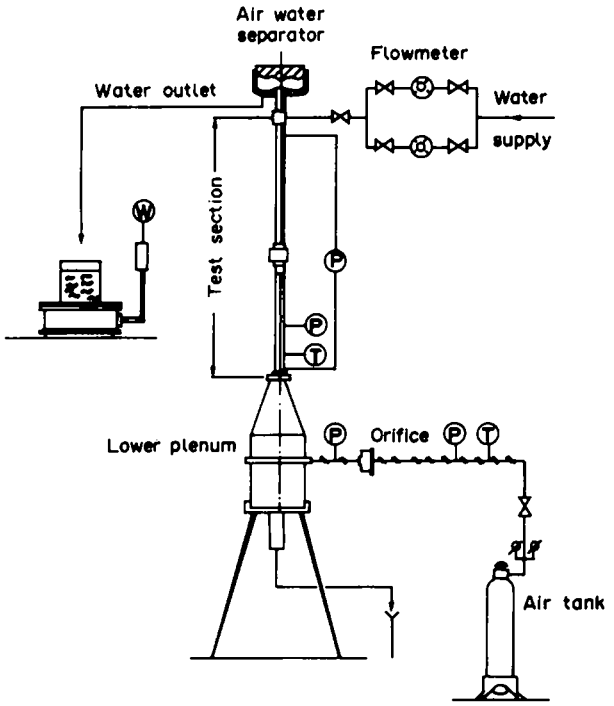

Figure 1. Schematic of the test loop.

RESULTS AND DISCUSSION

The first tests were performed to verify that the flooding curve did not change when alternatively keeping the liquid (or the gas) flow rate constant and increasing the gas (or the liquid) flow rate to reach the flooding condition. As shown in figure 2, where the gas superficial velocity, J_G, is plotted vs the inlet liquid superficial velocity, $J_{L,in}$ the experimental results lie on the same curve.

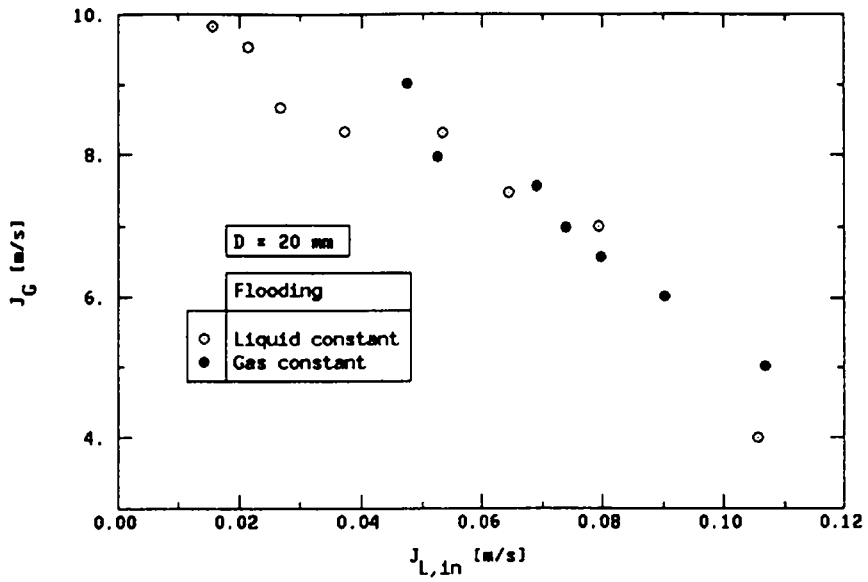

Figure 2. Gas superficial velocity at the onset of flooding, J_G, vs the inlet liquid superficial velocity, $J_{L,in}$; experimental procedures with either gas or liquid inlet constant flow rates.

The hysteresis results are plotted in figure 3, where the downwards delivered liquid superficial velocity, $J_{L,d}$, is reported vs $J_{L,in}$ for the 20 mm i.d. tube [see Celata *et al.* (1989) for the detailed experimental data set]. As shown in figure 3, the downwards delivered liquid flow rate becomes constant after the onset of flooding. Once this condition is reached, if the inlet liquid flow rate is decreased, the liquid flow rate at which countercurrent flow is restored corresponds to a value lower than the flooding liquid flow rate (deflooding point). The trend of the flooding–deflooding curves is similar if we reduce the tube diameter, D, as shown in figure 4.

A possible quantitative description of the phenomenon is given by introducing the "hysteresis factor", H, defined as follows:

$$H = \frac{J^*_{L,OF} - J^*_{L,DEF}}{J^*_{L,OF}}, \qquad [1]$$

where J^*_L is the Wallis parameter,

$$J^*_L = J_L\left[\frac{\rho_L}{gD(\rho_L - \rho_G)}\right]^{1/2}; \qquad [2]$$

J_L being the liquid superficial velocity (i.e. the volumetric flow rate divided by the cross section of the channel). The subscripts OF and DEF stand for "onset of flooding" and "deflooding point", respectively. The hysteresis factor ranges between 0 and 1; the value $H = 0$ corresponds to the condition of absence of hysteresis, which is typical for low values of the gas superficial velocity, while $H = 1$ represents the zero penetration condition, i.e. the condition when the downwards delivered liquid flow rate is zero and the deflooding point corresponds to the condition $J^*_L = 0$. In figure 5 the experimental values of H are plotted vs the non-dimensional gas velocity, J^*_G. The experimental trend shows a dependence of H on the channel diameter and gas velocity. From figure 5, it is possible to note that, for the limited set of available data, the functional dependence of H on J^*_G can be described by

$$H = \frac{1}{1 + A\exp(-BJ^*_G)}, \qquad [3]$$

where

$$J^*_G = J_G\left[\frac{\rho_G}{gD(\rho_L - \rho_G)}\right]^{0.5}. \qquad [4]$$

The parameter B may be assumed constant and equal to 9.5, whilst the parameter A is a function of the non-dimensional diameter:

$$D^* = D\left[\frac{g(\rho_L - \rho_G)}{\sigma}\right]^{0.5} \qquad [5]$$

In figure 5 the results obtained from [3] (——) are plotted assuming the following values for the parameter A:

$$A = 120.0 \quad \text{for} \quad D = 20.0\,\text{mm}, \quad D^* = 7.32$$
$$A = 19.5 \quad \text{for} \quad D = 16.2\,\text{mm}, \quad D^* = 5.92.$$

The lack of data for different diameters and fluids prevents us from defining a function $A = f(D^*)$ and testing the validity bounds of the observed phenomenon.

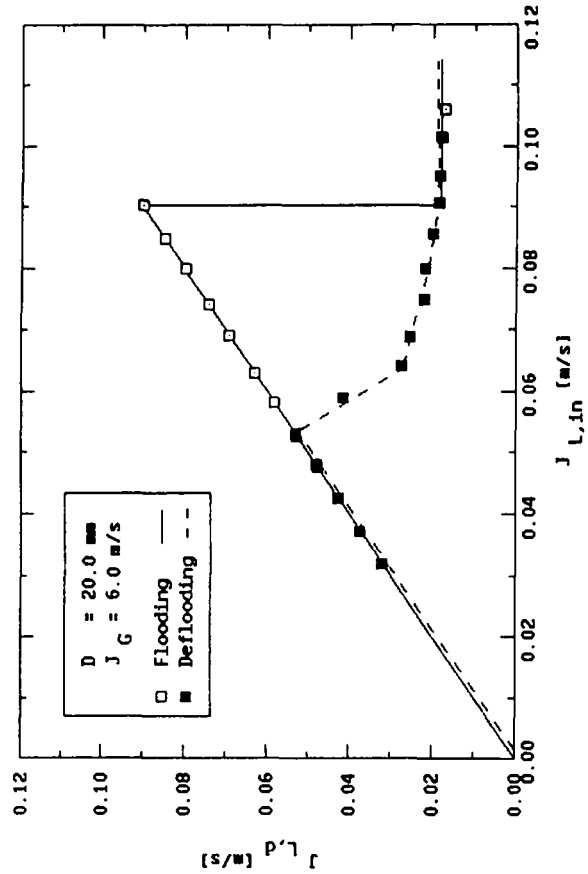
D = 20.0 mm
J G = 6.0 m/s
Flooding
Deflooding
J L,d [m/s]
J L,in [m/s]
0.00
0.02
0.04
0.06
0.08
0.10
0.12

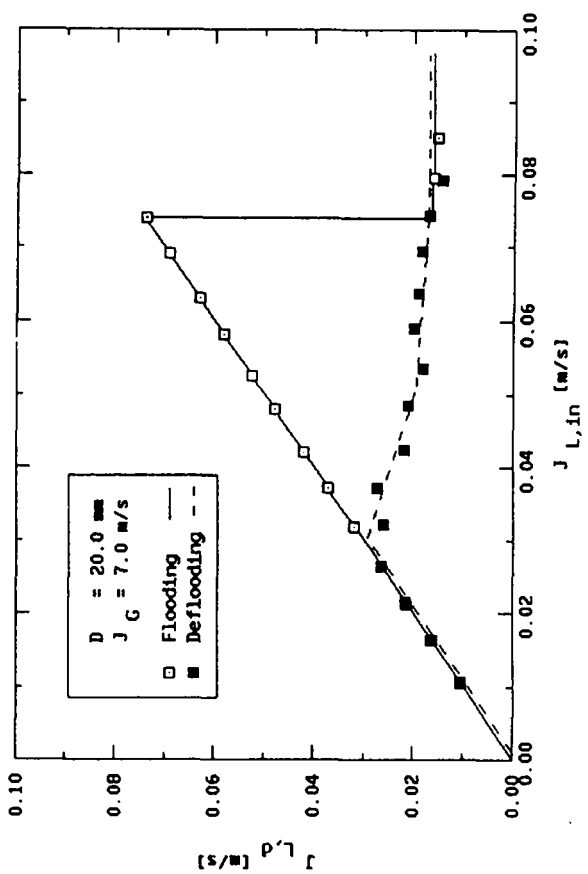
D = 20.0 mm
J G = 7.0 m/s
Flooding
Deflooding
J L,d [m/s]
J L,in [m/s]
0.00
0.02
0.04
0.06
0.08
0.10

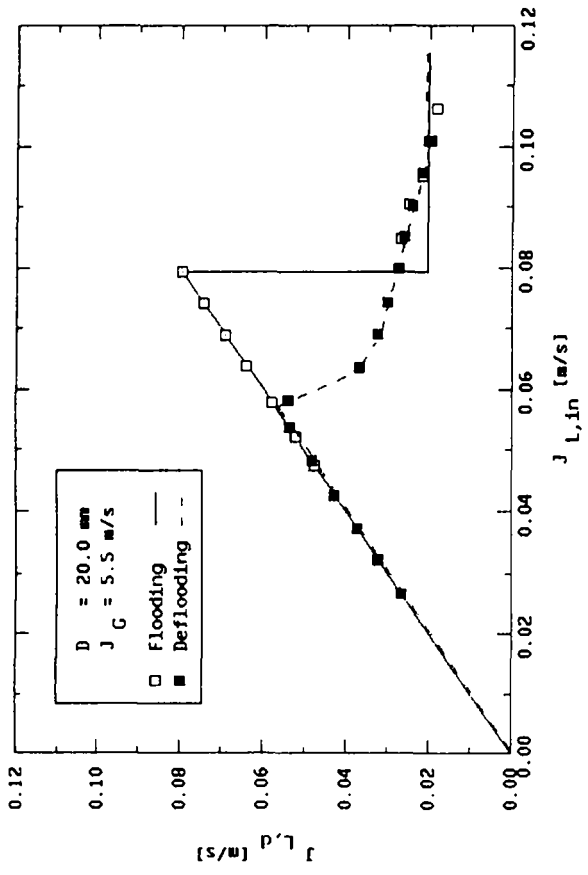
D = 20.0 mm
J G = 5.5 m/s
Flooding
Deflooding
J L,d [m/s]
J L,in [m/s]
0.00
0.02
0.04
0.06
0.08
0.10
0.12

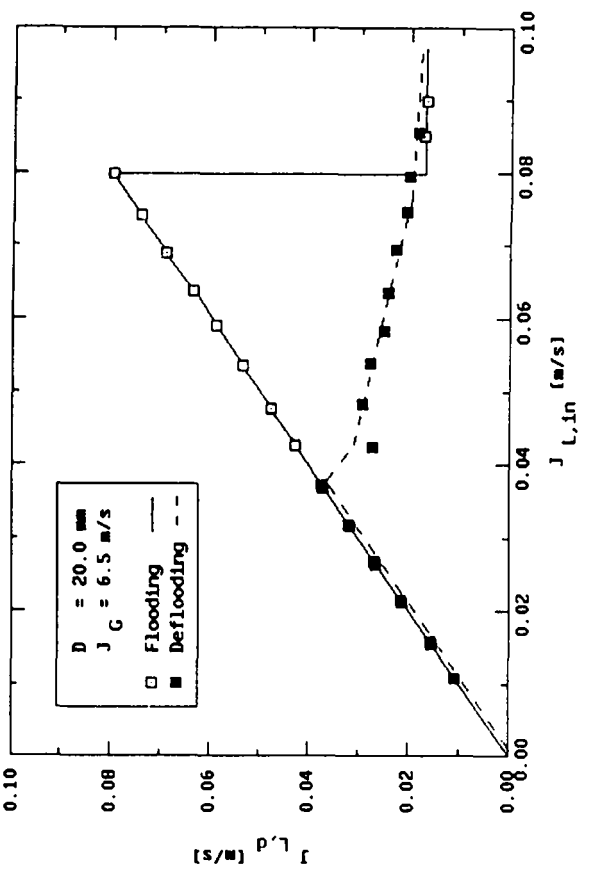
D = 20.0 mm
J G = 6.5 m/s
Flooding
Deflooding
J L,d [m/s]
J L,in [m/s]
0.00
0.02
0.04
0.06
0.08
0.10

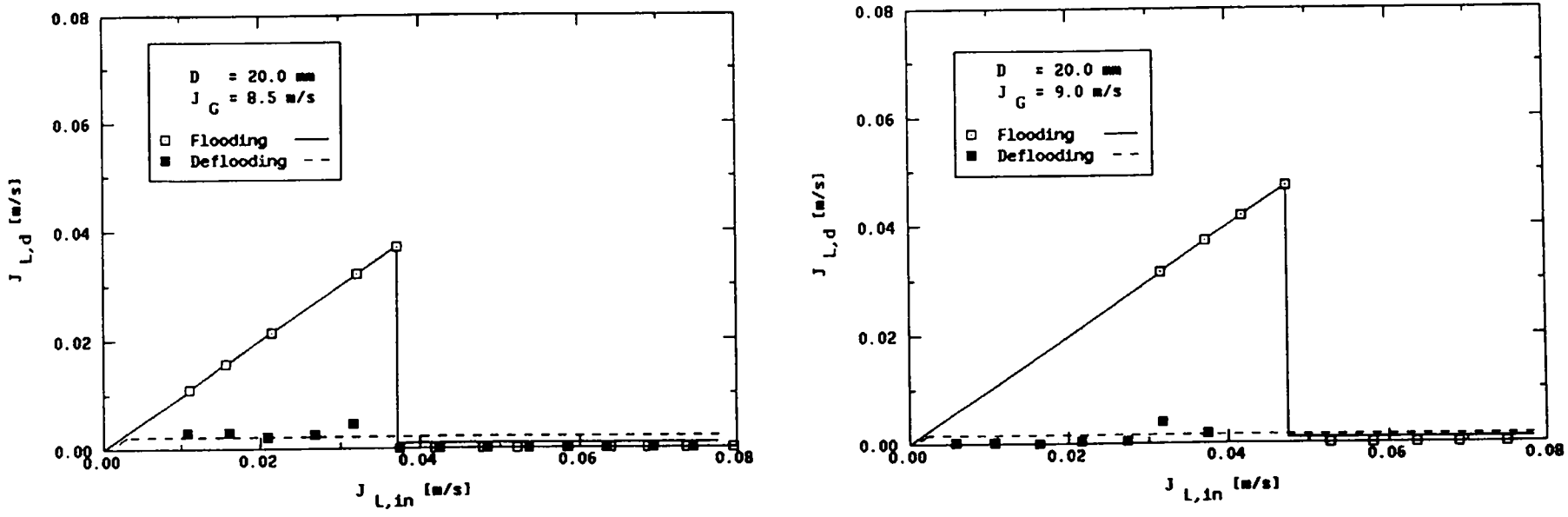

Figure 3. Hysteresis in 20 mm vertical pipes: downwards delivered liquid superficial velocity, $J_{L,d}$, vs the inlet liquid superficial velocity, $J_{L,in}$, for different nominal values of the inlet gas superficial velocity, J_G.

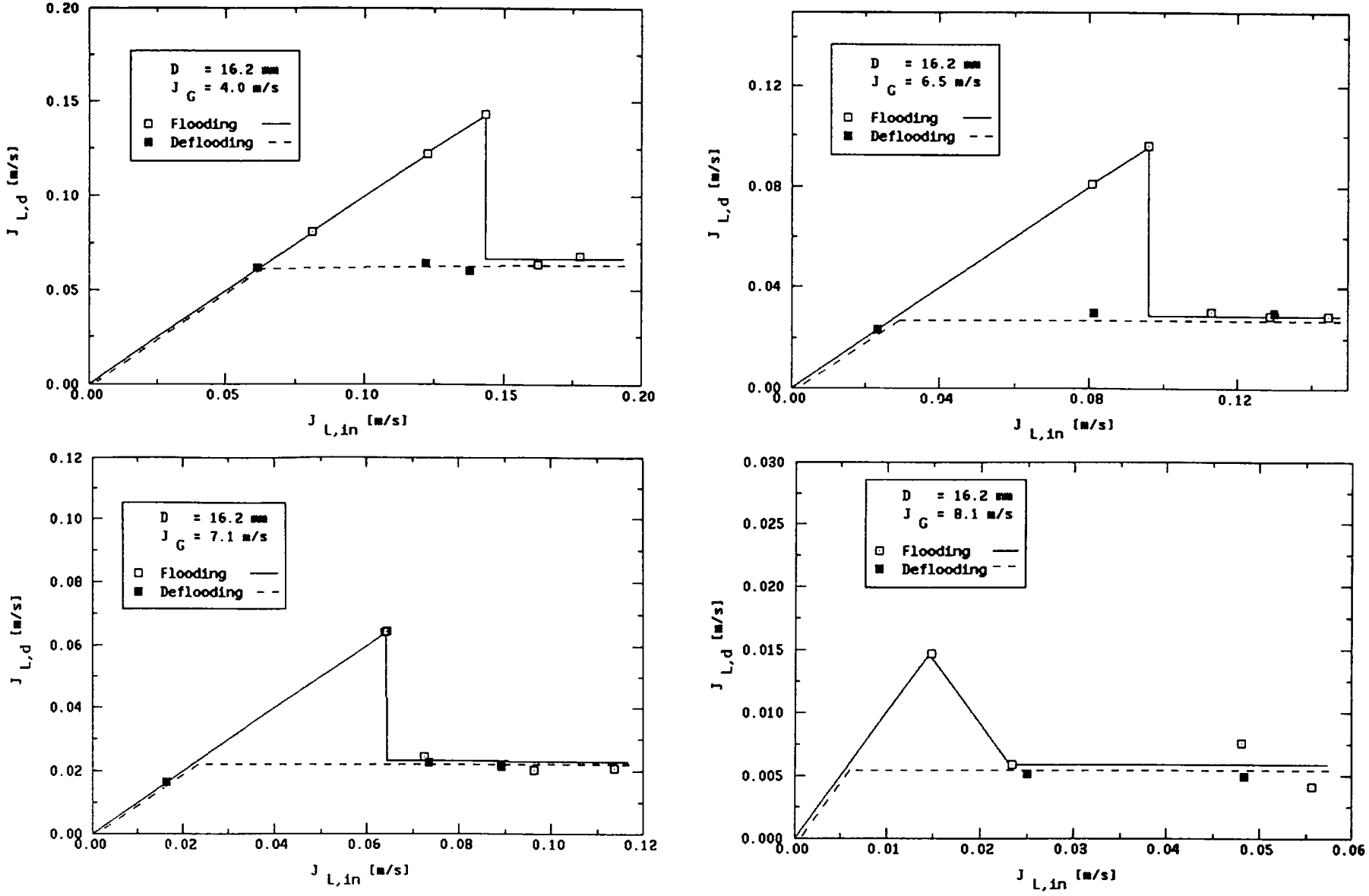

Figure 4. Hysteresis in 16.2 mm vertical pipes; downwards delivered liquid superficial velocity, $J_{L,d}$, vs the inlet liquid superficial velocity, $J_{L,in}$, for different nominal values of the inlet gas superficial velocity, J_G.

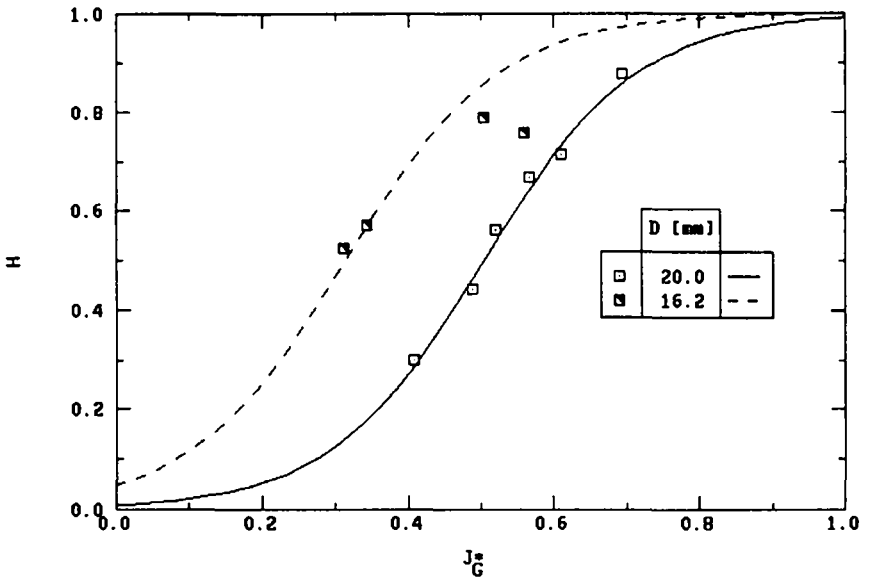

Figure 5. Representation of the hysteresis factor, H vs the non-dimensional gas superficial velocity, J_G^*.

REFERENCES

BECKER, K. M. & LETZTER, A. 1978 Flooding and deflooding measurement for counter current flow of air and water in vertical channels. Report KTH-NEL-25.

CELATA, G. P., CUMO, M., FARELLO, G. E. & SETARO, T. 1989 Analysis and "modelling" of flooding experiments: inclination, geometry, hysteresis, physical properties of fluids. ENEA Report No. NQDT-ITS4B-89068.

CLIFT, R., PRITCHARD, C. L. & NEDDERMAN, R. M. 1966 The effect of viscosity on the flooding conditions in wetted wall columns. *Chem. Engng Sci.* **21**, 87–95.

HEWITT, G. F. & WALLIS, G. B. 1966 Flooding and associated phenomena in falling film flow in a vertical tube. UKAEA Report AERE R-4022.